The 12th International Scientific Conference Intelligent Technologies in Logistics and Mechatronics Systems (ITELMS'2018), 26-27 April 2018, Panevėžys, Lithuania

第 12th 屆國際科學會議 智慧物流與機電系統技術（ITELMS'2018），2018 年 4 月 26–27 日，立陶宛帕涅韋日斯

Investigation of the Circle Fractal Structure Interaction with Gigahertz Frequency Electromagnetic Waves

圓形分形結構與吉赫茲頻率電磁波相互作用之研究

Dainius Jasaitis [a], Vaida Vasiliauskiene [a], Paulius Miškinis [a], Jovita Damauskaitė [a], Artūras Jukna [a*], Aleksandr Kopyltsov [b**], Genady Lukyanov [c], Konstantin Korshunov [d], Igor Serov [d]

Dainius Jasaitis [a]，Vaida Vasiliauskiene [a]，Paulius Miškinis [a]，Jovita Damauskaitė [a]，Artūras Jukna [a*]，Aleksandr Kopyltsov [b]，Genady Lukyanov [c]，Konstantin Korshunov [d]，Igor Serov [d]**

[a] Vilnius Gediminas Technical University, Sauletekio av. 11, Vilnius 10223, Lithuania

[a] 維爾紐斯格迪米納斯理工大學（Vilnius Gediminas Technical University），Sauletekio av. 11，Vilnius 10223，Lithuania

[b] Saint-Petersburg Electrotechnical University, Professor Popov str. 5, Staint-Petersburg 197376, Russia

[b] 聖彼得堡電工大學，Popov 街 5 號，聖彼得堡 197376，俄羅斯

[c] ITMO University, Kronverksky av. 49, Saint-Petersburg 197198, Russia

[c] ITMO 大學，Kronverksky 大道 49 號，聖彼得堡 197198，俄羅斯

dAIRES Human Genome Research Foundation, 61, Vyborgskaya nab., Saint-P

Abstract **摘要**

We present results of investigations of Si crystal (100) with a circularly periodic structure formed on its surface (resonatorconverter) interaction with low power radiation which can be attributed to electromagnetic pollution (EP). Due EP interaction with circularly periodic (diffraction grating) structure of the front/rear antennas and periodic structure of Si crystal our device in the regime of optical reflection can efficiently damp EP if incident power is ≥ 2 W. The efficiency of EP damping by means of our device is noticeably higher than that one of measured for a regular conducting plate of identical dimensions and orientation in the space. The results of our experimental measurements and model of power attenuation by the resonator-converter is presented and discussed.

我們呈現了對在矽晶體 (100) 表面形成之圓形周期結構（諧振器-換能器）與可歸類為電磁汙染（EP）之低功率輻射間交互作用的研究結果。由於 EP 與前 / 後天線的圓形周期（繞射光柵）結構以及矽晶體的周期結構發生相互作用，使得本裝置在光學反射工作模式下能有效衰減入射功率為 ≥ 2 W 的 EP。以本裝置衰減 EP 的效率明顯高於對具有相同尺寸及朝向的常規導電金屬板所測得之效率。我們提出並討論了實驗測量結果與諧振器-換能器之功率衰減模型。

Peer-review under responsibility of the Kaunas University of Technology, Panevėžys Faculty of Technologies and Business

同行審查由考納斯理工大學潘艾韋贊尼斯（Panevėžys）科技與商業學院負責

Keywords: fractal antenna, electromagnetic polution, optical reflection, optical transmission, diffraction grating

關鍵詞：分形天線、電磁汙染、光學反射、光學透射、繞射光柵

1. Introduction **1. 引言**

All organic and inorganic objects in nature are constantly being exposed to a natural electromagnetic radiation (EMR) produced by the cosmic radiation [1] (the biggest part of it is absorbed by the Earth atmosphere), emitted by the Earth's crust (due to nuclear reactions of radioactive elements in it), and coming from artificial sources in the highly urbanized and/or domestic industry environment. In fact, humankind, animals and plants use EMR for a variety of their living activities, like those of telecommunication, control and regulation of their various behavioral and physiological functions. However, though essential for living objects, exposure to excess low frequency (equal or higher than 50 Hz) [2,3] and/or high frequency (below 2.5 GHz) EMR beyond the naturally evolved tolerance limits can cause various human illnesses [2] and/or harmful biological effects in humans' bodies [4,5].

自然界中所有有機與無機物體持續暴露於自然電磁輻射（EMR），該輻射由宇宙輻射產生[1]（其中大部分被地球大氣吸收）、由地殼放射性元素進行核反應所發出的輻射，以及來自高度都市化與/或家庭工業環境中的人工來源所發出。事實上，人類、動物與植物在多種生命活動中利用電磁輻射，例如通訊、控制與調節各種行為與生理功能。然而，儘管電磁輻射對生物體至關重要，超出自然演化耐受限度的過量低頻（等於或高於 50 Hz）[2,3]及/或高頻（低於 2.5 GHz）電磁輻射，仍可能造成各種人類疾病[2]及/或對人體產生有害的生物效應[4,5]。

The artificial sources of ambient non-ionizing electromagnetic pollution (EP) are power supply lines (the higher the voltage, the higher radiation power), microwaves and radars, telecommunication equipment/devices and electrical appliances, radio and TV signals transmitters, even computers and their monitors, electric clocks, heated waterbeds, blankets etc. All together these sources create surrounding us EP with frequency of EMR ranging from 0 Hz (static electromagnetic field) to 300 GHz (microwaves and millimeter waves). The effects of extremely lowfrequency EMR are dependent on dose and duration of exposure and are cumulative. Therefore, todays humankind start asking questions how to assess the exposures to the human body from EP and to protect them from excess of EMR which can lead to cells and/or neurons damage or even damage to chromosomes altering the structure of our DNR [6].

人為來源的環境非電離電磁污染（EP）包括電力供應線（電壓越高，輻射功率越大）、微波與雷達、電信設備 / 裝置與電器、無線電與電視訊號發射器，甚至電腦及其顯示器、電鐘、加熱水床、毯子等。這些來源共同產生包圍我們的電磁污染，其電磁輻射頻率範圍從 0 Hz（靜電磁場）到 300 GHz（微波與毫米波）。極低頻電磁輻射的影響取決於劑量與暴露持續時間，且具有累積性。因此，當代人類開始提出如何評估人體受到的電磁污染暴露，以及如何保護人體免於過量電磁輻射的問題，因為過量可能導致細胞及 / 或神經元受損，甚至損害染色體，改變我們 DNA 的結構[6]。

Protecting themselves from EP one can simply limit time period of direct contact with electronic appliances, but technically it is difficult to accomplish in nowadays living/working environment, be aware of high power radiation sources what is almost impossible in highly urbanized/industrial areas, or use electromagnetic shields which potentially can increase immunity of the shielded device and decreases the power of undesirable radiation from it [7]. Moreover, the electronic appliances emit power from a number of primary and secondary sources and their emissions become an uncorrelated broadband EP which can be totally suppressed only by means of the signals phasor addition for all contributions resulting the radiation field.

要保護自己免受電磁污染（EP）的影響，人們可以簡單地限制與電子設備直接接觸的時間，但在現今的生活/工作環境中技術上很難做到；也可注意高功率的輻射來源，但在高度都市化/工業化地區這幾乎不可能；或使用電磁屏蔽，這有可能提高被屏蔽裝置的抗干擾能力並降低其不希望有的輻射強度 [7]。此外，電子設備會從多個主要與次要來源發射能量，而它們的輻射會變成非相關的寬頻電磁污染，只有透過對所有構成輻射場的貢獻進行訊號相量相加，才能將其完全抑制。

Our work aims on experimental testing of a silicon crystalline (100) resonator-converter interaction with low power $0.9-2.5\mathrm{GHz}$ frequency continuous wave signals which frequency can be attributed to frequency range of ambient non-ionizing EP. The resonator-converter (device) is shaped in a form of circular diffraction grating with a variable period starting with 0.001 mm wide "slits" at the device's centre and ending with 0.1 mm wide "slits" at the Si crystal edges and consists of front and rear antennas which are also circularly periodic diffraction gratings spaced by a $1-\mathrm{mm}$-thick insulator ($\varepsilon=3.5@10\mathrm{GHz}-4@2.5\mathrm{GHz}$) [8] located in between them. Our results of experimental investigation show that the resonator-converter suppresses power of incident EMR and, due to incident wave interference with a wave reflected from device's surface, it retransforms the incident EMR in terms of frequency/wavelength and phase. Our experimental results of incident power suppression when our device is operating at room temperature in the regime of

optical reflection and in the regime of optical transmission are presented and discussed.

我們的工作旨在實驗測試一個矽單晶(100)諧振器-轉換器與低功率 $0.9-2.5\mathrm{GHz}$ 頻率連續波訊號的相互作用，該頻率可歸屬於環境非電離電磁場的頻率範圍。該諧振器-轉換器（裝置）呈圓形繞射光柵形狀，具可變週期，從裝置中心 0.001 mm 寬的「裂縫」開始，至矽晶片邊緣 0.1 mm 寬的「裂縫」結束，並由前、後兩個天線構成，這兩個天線亦為圓形週期性繞射光柵，兩者之間由厚度為 $1-\mathrm{mm}$ 的絕緣層（ $\varepsilon=3.5@10\mathrm{GHz}-4@2.5\mathrm{GHz}$ ）[8] 隔開。實驗研究結果顯示，該諧振器-轉換器抑制入射電磁輻射的功率，並且由於入射波與從裝置表面反射波的干涉，它在頻率/波長與相位方面重新轉換入射的電磁輻射。本文呈現並討論了當本裝置在室溫下分別於光學反射及光學透射工作模式時，入射功率被抑制的實驗結果。

2. Samples and measurement setup

2. 樣品與測量配置

Our tested resonator-converter (device) contains a $500-\mu\mathrm{m}$-thick round shaped $\mathrm{Si}(100)$ crystal plate glued onto surface of a front antenna (Fig 1 on the left) which physical shape defined as a fourth iteration circle fractal. The surface of Si crystal plate modified by means of plasma-chemical etching of $600-\mathrm{nm}$-deep and $600-\mathrm{nm}$-wide groves which produce a net of intercrossing rings (Fig. 1 on the right). Since etched groves on the silicon surface affects a periodic change in crystal's thickness, the crystal behaves like a diffraction grating with a variable period produced by intercrossing rings of the fourth iteration circle fractal with a diameter of $D_1=7.5\ \mathrm{mm}$. It means that for every further step of iteration the diameter of rings decreases proportionally to ratio $D_2=D_1/2, D_3=D_2/2$, and $D_4=D_3/2$ in such a way producing a diffraction grating of a variable period (Fig. 1 on the right).

我們測試的諧振器-轉換器（裝置）包含一片厚度為 $500-\mu\mathrm{m}$ 的圓形 $\mathrm{Si}(100)$ 晶片，黏貼在前天線的表面（圖 1 左側），其物理形狀定義為第四次迭代的圓形分形。矽晶片表面經由等離子化學蝕刻製成深度為 $600-\mathrm{nm}$ 、寬度為 $600-\mathrm{nm}$ 的溝槽，形成相互交錯的環狀網絡（圖 1 右側）。由於矽表面的蝕刻溝槽造成晶片厚度呈週期性變化，該晶片表現得如同一個具可變周期的繞射光柵，該可變周期由第四次迭代圓形分形的交錯環所產生，環的直徑為 $D_1=7.5\ \mathrm{mm}$ 。這表示每進一步的一次迭代，環的直徑按比例縮小，比例為 $D_2=D_1/2, D_3=D_2/2$ ，並以 $D_4=D_3/2$ 的方式產生可變周期的繞射光柵（圖 1 右側）。

The circles of groves on the surface of Si plate form a circularly periodic topology of the Si resonator-converter, which is fixed on a top of front antenna (Fig. 1. on the left). Two identical antennas, the front and rear, in our device

矽片表面的環狀溝槽在矽諧振器-轉換器上形成圓周周期性的拓樸結構，該諧振器固定在前天線的頂端（圖 1 左側）。在我們的裝置中，前後兩個天線是相同的，

are used for receiving ultra-wide band frequency continuous-wave EMR with the frequency band ranging between 0.9 and 2.5 GHz frequencies, which can be attributed to frequency range of ambient non-ionizing EP. The front and rear conducting (metallic) antennas are also manufactured as diffraction gratings produced by $0.1-\mathrm{mm}$-thick and $0.1-$ mm -wide intercrossing rings of metal fourth iteration fractal of the circle with a diameter of $D_1=12.5\ \mathrm{mm}$ with a diameter of rings of every further step of iteration following ratio $D_2=D_1/2, D_3=D_2/2$, and $D_4=D_3/2$ in such a way producing a diffraction grating (Fig. 1 on the right) of a variable period ranging from several millimeters down to tens of micrometers.

用於接收超寬頻連續波電磁輻射（EMR），頻段介於 0.9 至 2.5 GHz，可歸因於環境非電離電場（EP）的頻率範圍。前後的導電（金屬）天線亦以繞射光柵製成，該光柵由厚度為 $0.1-\mathrm{mm}$ 、寬度為 $0.1-$ 毫米的金屬互相交錯環組成，採用直徑為 $D_1=12.5\ \mathrm{mm}$ 的圓形四階分形，每一步迭代的環直徑依比率 $D_2=D_1/2, D_3=D_2/2$ 與 $D_4=D_3/2$ 逐級縮減，從而產生一個繞射光柵（右圖，圖 1），其可變週期範圍從數毫米到數十微米不等。

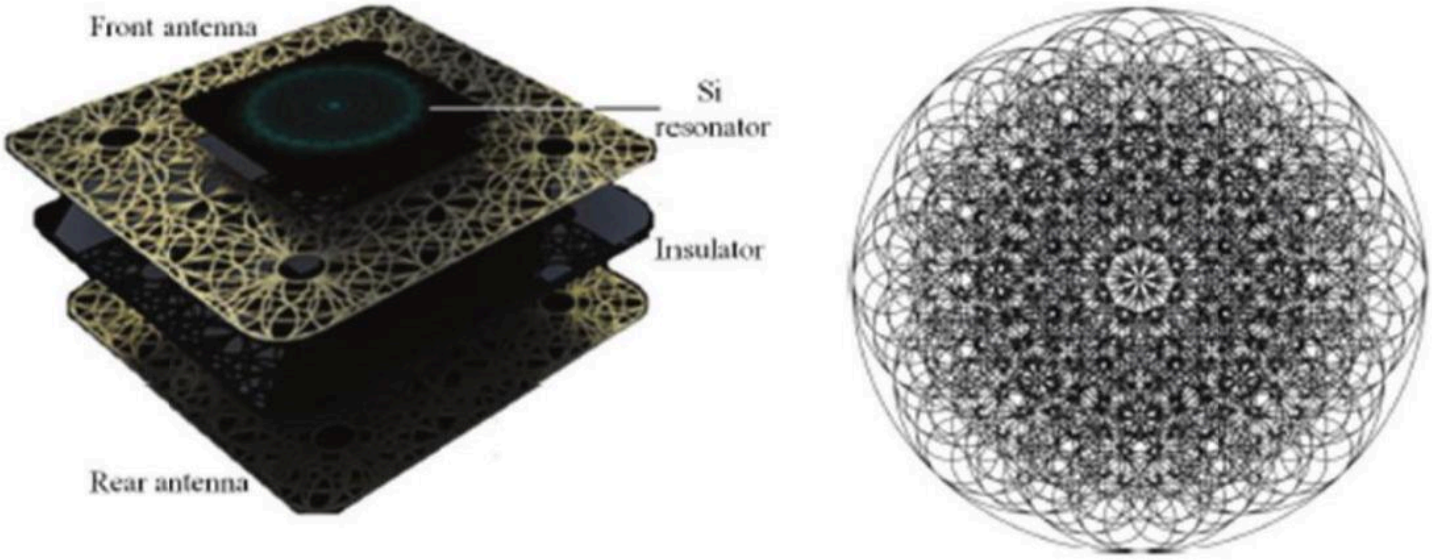

\captionsetup{labelformat=empty}
Figure 1: Fig. 1. Schematics of the resonator-converter consisting of a silicon resonator fixed on the top of the front antenna (on the left) and a schematic sketch of plasma-chemically etched groves on its surface (on the right). Similar design of the fourth iteration circle fractal (on the right) has been applied for the front and rear antennas of this device

圖 1：圖 1。諧振器－轉換器的示意圖，顯示固定在前天線頂端的矽諧振器（左）與其表面經等離子化學蝕刻形成的溝槽示意（右）。相同設計的第四階圓形分形（右圖）已應用於本裝置的前後天線。

The equivalent circuit of the resonator-converter is a capacitor comprising two conductive electrodes separated by an insulator. The interaction of the capacitor with incident EM wave results in charging up of the capacitor C and the device's antenna gain depends of antenna impedance given by $(L_p/C)^{1/2}$ where L_p stands for the parasitic inductance of both metallic antennas and of the Si resonator.

諧振器-轉換器的等效電路是一個由兩個導電電極以絕緣體隔開所構成的電容器。該電容器與入射電磁波的相互作用導致電容被充電 C ，而裝置的天線增益取決於天線阻抗，該阻抗由 $(L_p/C)^{1/2}$ 給出，其中 L_p 代表兩個金屬天線以及矽諧振器的寄生電感。

Our measurement setup consists of continuous-wave signals generators (for this purpose we have been using different radiation sources of household appliances), emitting wide band signals in frequency band ranging between 0.9 GHz and 2.5 GHz and of resonator-converter. For signals detection we used the Signal Hound Spectrum analyzer receiving signals in the $0-8\mathrm{GHz}$ frequency band. The signals were detected in the near-field (the resonator-converter located close to radiation source) and in the far-field (the resonator-converter located at distance $L > 10\lambda$) zones. Here λ is the wavelength of the central frequency of the signal received by the signals detector.

我們的測量配置由連續波信號發生器組成（為此我們使用了家庭電器等不同的輻射源），在 0.9 GHz 至 2.5 GHz 之間發射寬頻信號，並配合諧振器-轉換器。為了偵測信號，我們使用了 Signal Hound 頻譜分析儀，接收 $0-8\mathrm{GHz}$ 頻段的信號。信號在近場（諧振器-轉換器靠近輻射源）及遠場（諧振器-轉換器位於距離 $L > 10\lambda$ ）區域被偵測。此處 λ 為信號偵測器接收之信號中心頻率的波長。

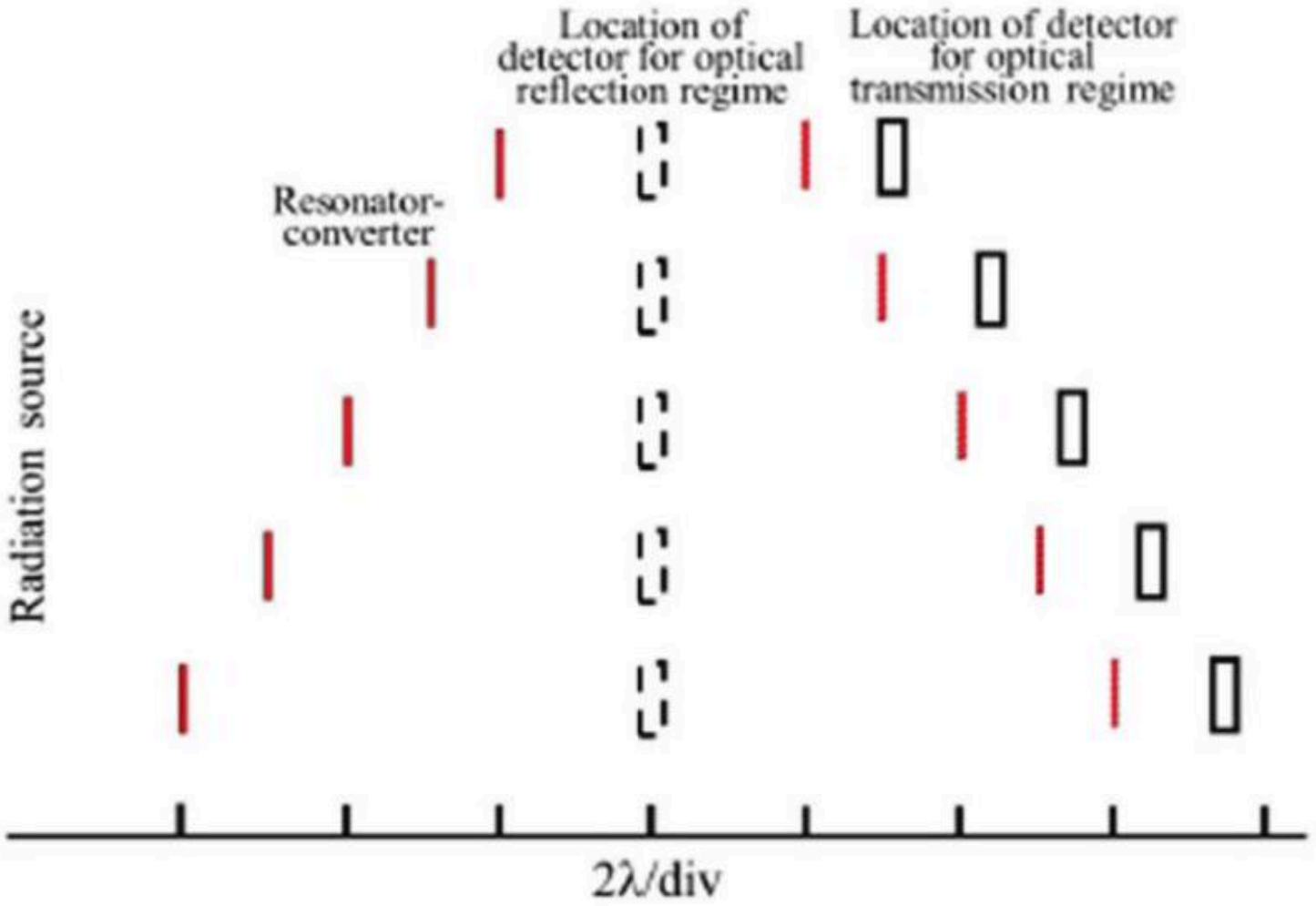

\captionsetup{labelformat=empty}
Figure 2: Fig. 2. A scheme explaining experimental setup for detection of signals when the resonator-converter is used in a regime of optical reflection (dashed lines) and in the regime of optical transmission (solid lines) and distances between radiation source, detector, and the resonator-converter are given in λ-as. Here λ is the wavelength of the central frequency of the source radiated wave

圖 2：圖 2。說明在諧振器-轉換器用於光學反射模式（虛線）與光學透射模式（實線）時信號偵測實驗佈置的示意圖，並標示了輻射源、探測器與諧振器-轉換器之間的距離，用 λ 表示。此處 λ 為輻射源發射波中央頻率的波長

We measured power of $0.9 - 2.5\mathrm{GHz}$ electromagnetic waves (in dBm) transmitted through the resonatorconverter (the regime of optical transmission (Fig. 2)) and that of reflected waves from our device (the regime of optical reflection) in the near-field and far-field zones of the resonator-converter and then the power values were converted into electric field amplitude, presuming that radiation sources are ideal electric dipoles with antenna gain of 2.15 dBi . For the optical reflection measurements, our detector of radiation we located in between radiation source and resonator-converter in the near-field and far-field zones. The power of detected signal was analyzed by means of the FFT method sampling the detected signal over a period of time and measuring amplitudes of its frequency components.

我們測量了經過諧振器-轉換器傳輸的 $0.9 - 2.5\mathrm{GHz}$ 電磁波（以 dBm 為單位）（光學透射模式（圖 2））以及從裝置反射出的波（光學反射模式）在諧振器-轉換器近場與遠場區域的功率，然後將功率值換算為電場振幅，假定輻射源為天線增益為 2.15 dBi 的理想電偶極子。對於光學反射測量，我們將輻射探測器置於輻射源與諧振器-轉換器之間的近場與遠場區域。偵測到的信號功率以 FFT 方法分析，透過對偵測信號在一段時間內取樣並測量其頻率成分的振幅來進行。

To calculate experimental mean values all measurements either under laboratory or field conditions were repeated for several times at fixed distances between the resonator-converter and the detector given in λ-as. Four different radiation sources transmitting 0.5 W@0.9GHz (No. 1), 2 W@0.9GHz (No. 2), 400 W @ 2.5 GHz (No. 3), and 800 W @ 2.5 GHz (No. 4) we used for our measurements. However, to minimize errors of our experimental measurements, in current report we

will mainly focus on experimental results using the most powerful radiation source No. 4.

為了計算實驗平均值，所有在實驗室或田間條件下的測量皆在諧振器-轉換器與探測器之間保持固定距離的情況下重複進行多次，距離以 λ -as 表示。我們使用了四種不同的輻射源進行測量，分別為發射 0.5 W@0.9GHz （編號 1）、 2 W@0.9GHz （編號 2）、400 W @ 2.5 GHz（編號 3）與 800 W @ 2.5 GHz（編號 4）。然而，為了將實驗測量的誤差降到最低，在本報告中我們將主要著重於使用最強輻射源編號 4 的實驗結果。

3. Measurement results and discussion

3. 測量結果與討論

3.1. Experimental results

3.1. 實驗結果

EMR interaction with the resonator-converter has been studied by means of detection of residual signal power versus distance between the detector and a radiation source in the case when the resonator-converter operates in the regime of optical transmission. Figure 3 represents difference in electric field amplitudes $E_0 - E_1$ versus distance of the detector from mentioned above four types of radiation sources. Here E_0 stands for electric field amplitude of radiation source emitted signal and E_1 is the residual electric field amplitude transmitted through the resonatorconverter which was located in the near-field zone of radiation source.

通过在諧振器-轉換器於光學透射模式下操作時，測量偵測器與輻射源之間距離與殘餘訊號功率的關係，來研究電磁輻射（EMR）與諧振器-轉換器的相互作用。圖 3 顯示了在上述四種輻射源情況下，偵測器與輻射源距離變化時電場振幅差 $E_0 - E_1$ 的變化。其中 E_0 代表輻射源所發射訊號的電場振幅，而 E_1 則為通過位於輻射源近場區的諧振器-轉換器所傳輸出的殘餘電場振幅。

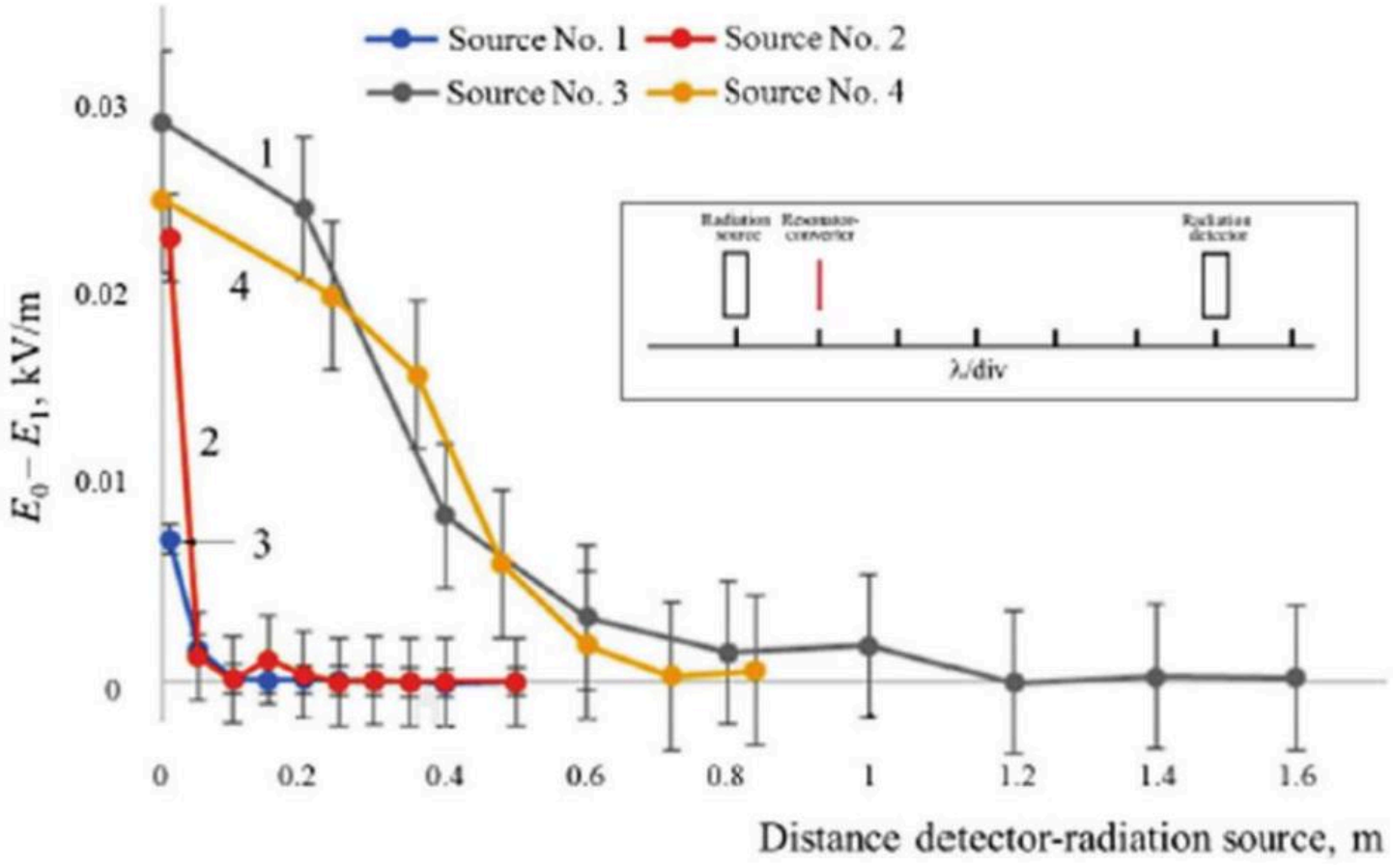

\captionsetup{labelformat=empty}
Figure 3: Fig. 3. A plot of difference of electric field amplitudes ($E_0 - E_1$) recorded by the signals detector versus distance detector-radiation source. Here E_0 is electric field amplitude of the source emitted signal and E_1 is electric field amplitude of the signal transmitted through the resonator-converter which was fixed in the near-field zone of the radiation source. Numbers and colors of curves in the graph represent results of experimental measurements using four different sources of

EMR. Inset represents a schematic of our measurement setup

圖 3：圖 3。偵測器記錄的電場振幅差（$E_0 - E_1$）相對於偵測器—輻射源距離的圖示。此處 E_0 為來源發射訊號的電場振幅，E_1 為固定在輻射源近場區之諧振器-轉換器所傳輸訊號的電場振幅。圖中曲線的編號與顏色代表使用四種不同電磁輻射源進行實驗測量的結果。插圖為我們測量裝置的示意圖。

The electric field amplitude of the transmitted through the resonator-converter gigahertz frequency EMR decreased by $\sim 27\%$ (i.e. electric field amplitude damping ratio -2.07 dB) level on average in whole range of our tested distances from the radiation source No. 4 (Fig. 3, curve 1 (grey)). Here and in all other experimental cases the resonator-converter is attached directly to the frame of a radiation source, i.e. located in its near-field zone.

通过谐振器–轉換器傳輸的吉赫頻率電磁輻射的電場振幅在我們測試的來自輻射源 No. 4 的整個距離範圍內平均下降了 $\sim 27\%$（即電場振幅衰減比 -2.07 dB）（圖 3，曲線 1（灰色））。在此以及所有其他實驗情況中，諧振器–轉換器皆直接附著於輻射源框架上，即位於其近場區域。

Increasing distance from the radiation source, the parameter $E_0 - E_1$ gradually decreased and finally vanished at distance 1.2 m (curve 1), 0.85 m (curve 4) and at distances below 0.2 m (curves 2 and 3).

隨著與輻射源距離的增加，參數 $E_0 - E_1$ 逐漸減小，最終在距離 1.2 m（曲線 1）、0.85 m（曲線 4）以及在低於 0.2 m 的距離（曲線 2 和 3）處消失。

All curves in Figure 3 show strongly nonlinear behavior with increasing detector's distance from the radiation source and this feature let us to predict that the lever of power damping by the resonator-converter should depend on power of incident EMR. Since our tested radiation, sources are not zero-dimensional and in all cases amplitude and frequency range of radiation is a result of superposition of radiation of several primary and secondary sources, the electric field amplitude of 800 W radiation source does not decrease with increasing distance squared. However, the variation of the parameter $E_0 - E_1$ show that the resonator-converter turns-on at high power and turns-off when the incident power appears to be below some threshold value $P_{\min}$. As it follows from our measurement results the minimum power required for turning-on the resonator-converter is of order of $P_{\min} \sim 2$ W (curve 2 (red)). Our preliminary results also show that $P_{\min}$ is a function of frequency/wavelength of an incident electromagnetic wave and $P_{\min}$ decreasing with increasing central frequency of an incident EMR.

圖 3 中的所有曲線顯示出隨偵測器與輻射源距離增加而強烈的非線性行為，這一特性讓我們預測，諧振器-轉換器對功率的阻尼程度應該依賴於入射電磁輻射的功率。由於我們測試的輻射源並非零維，在所有情況下，輻射的振幅與頻率範圍都是多個主要與次級源輻射疊加的結果，因此 800 W 輻射源的電場振幅並不隨距離平方而減小。然而，參數 $E_0 - E_1$ 的變化顯示諧振器-轉換器在高功率時會啟動，而當入射功率低於某個閾值 $P_{\min}$ 時則會關閉。正如我們的測量結果所示，使諧振器-轉換器啟動所需的最小功率約為 $P_{\min} \sim 2$ W（曲線 2（紅色））。我們的初步結果也顯示 $P_{\min}$ 是入射電磁波頻率 / 波長的函數，且 $P_{\min}$ 會隨入射電磁輻射的中心頻率增加而減小。

The electric field amplitude of 800 W power radiation source versus distance to the signals detector is shown in Fig 4 on the left (here the resonator-converter used in the regime of optical transmission) and in Figure 4 on the right (the regime of optical reflection). In both experimental cases, the distance between the resonator-converter and signals detector was kept constant while the detector moves away from the radiation source.

800 W 輻射源的電場振幅與信號偵測器之間距離的關係如圖 4 左側所示（此處共振器-轉換器在光學透射模式下使用），以及圖 4 右側所示（光學反射模式）。在兩種實驗情況中，共振器-轉換器與信號偵測器之間的距離保持不變，同時偵測器遠離輻射源移動。

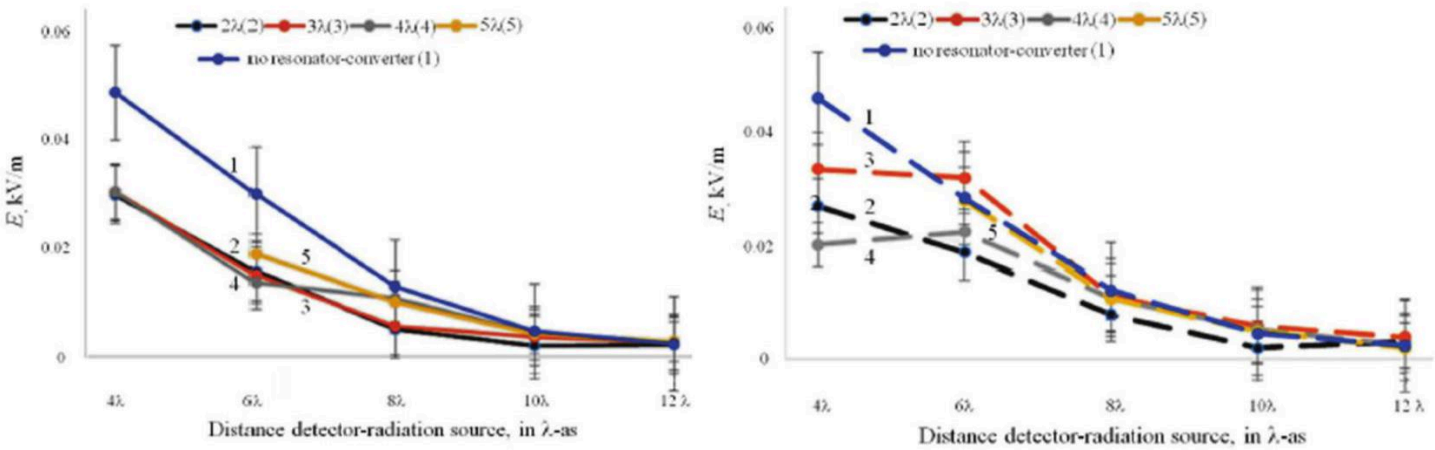

\captionsetup{labelformat=empty}
Figure 4: Fig. 4. The electric field strength detected at various distances (in λ-as) from an 800 W radiation source. Here figure (on the left) represents the case when our tested resonator-converter used in the regime of optical transmission and figure (on the right) when the resonator-converter used in the regime of optical reflection. In both experimental cases the distance between the resonator-converter and detector is fixed at 2λ (curve No. 2), $3\lambda(3)$, $4\lambda(4)$, and $5\lambda(5)$ (see figure legends) while the detector moves away from the radiation source. Here $\lambda = 12$ cm is the wavelength of the central frequency of the source radiated signals

圖 4：圖 4. 在距離 800 W 輻射源不同距離（以 λ 為單位）處偵測到的電場強度。此處左圖代表我們測試的共振器-轉換器在光學透射模式下的情況，右圖則為共振器-轉換器在光學反射模式下的情況。在兩種實驗中，共振器-轉換器與偵測器之間的距離固定為 2λ（曲線編號 2）、$3\lambda(3), 4\lambda(4)$ 與 $5\lambda(5)$（見圖例），而偵測器則遠離輻射源移動。此處 $\lambda = 12$ cm 為輻射源所發信號中心頻率的波長。

The electric field amplitude of the transmitted through the resonator-converter EMR decreases considerably (Fig. 4 on the left), however the parameter $E_0 - E_1$ (it was calculated by subtracting curves Nos. 2-5 from curve No. 1 in figure) does not depend on the resonator-converter distance from the detector. Slightly weaker damping of the electric field amplitude, but very similar behavior of the parameter $E_0 - E_1$ with increasing distance from the detector demonstrates the conductive (metallic) plate when we substituted it for the resonator converter. Having same dimensions as the resonator-converter the metallic plate in our measurement setup exhibited effect of electromagnetic screening of EMR electric field component demonstrating $7 - 8$ percent lower level of EMR damping if compare it with that one of the resonator-converter.

通过共振器-轉換器傳輸的電場振幅明顯減小（左圖 4），然而參數 $E_0 - E_1$（在圖中通過將曲線 №2–5 從曲線 №1 中相減計算得出）並不取決於共振器-轉換器與探測器之間的距離。當我們用導電（金屬）板替換共振器-轉換器時，電場振幅的阻尼略弱一些，但參數 $E_0 - E_1$ 隨距離增加的行為非常相似。與共振器-轉換器具有相同尺寸的金屬板在我們的測量配置中展現出對電磁輻射電場分量的電磁屏蔽效應，與共振器-轉換器相比，其電磁輻射阻尼水平低 $7 - 8$ 百分點。

When the resonator-converter operated in the regime of optical reflection (Fig. 4 on the right), the maximal damping of electric field amplitude we observed for the distances between the resonator-converter and the detector lower or equal to 2λ or when the resonator-converter attached to the frame of the detector. These results let us to conclude that most efficient damping of the EP could be expected when the resonator-converter operates in regime of the optical reflection and when incident EMR power is greater or equal to $P_{\min}$.

當諧振器-轉換器在光學反射模式下運作時（右圖 4），我們觀察到當諧振器-轉換器與探測器之間的距離小於或等於 2λ 或當諧振器-轉換器附著於探測器框架上時，電場振幅的最大阻尼。這些結果使我們得出結論：當諧振器-轉換器在光學反射模式下運作且入射電磁輻射功率大於或等於 $P_{\min}$ 時，可預期對電場強度（EP）的阻尼最為有效。

3.2. Results of numerical simulation

3.2. 數值模擬結果

Our results of numerical simulation of the resonator-converter interaction with an incident monochromatic wave of 550 THz frequency showed that 5.75 cm in diameter and 1 mm thick Si crystal modified surface by means of plasma-chemically etched $0.5 - \mu$m-wide and $0.5 - \mu$m-deep grooves undergoes non-uniform distribution of free carriers. An incident EMR charges up Si crystal producing stronger electric field (i.e. inducing larger concentration of free carriers) between the bottom of grooves located on a top of the silicon crystal and crystal's bottom surfaces. We simulated both the redistribution free-carrier concentration along the Si crystal surface and a strength of the electric field in the near-field zone of this crystal. Our results showed that high concentration of free-carriers collected in the grooves of the Si crystal can initiate a spontaneous electric discharge causing the electric field strength redistribution and flow of electric current along the resonator-converter surface [9]. It means that for the most efficient damping of EP of specific frequency range the doping of Si crystal (i.e. its electric conductivity) of the resonator-converter has to be optimized. It is also demonstrated that efficiency of the EMR damping by the resonator-converter is a function of Si crystal and metallic antennas topology as well as

characteristic frequency/wavelength of an incident EMR.

我們對一個直徑 5.75 公分、厚度 1 毫米的矽(Si)晶體，其表面經由等離子化學蝕刻出寬度為 $0.5-\mu\mathrm{m}$ 、深度為 $0.5-\mu\mathrm{m}$ 的溝槽時，與入射頻率為 550 THz 的單色波之共振器-轉換器相互作用所做的數值模擬結果顯示，游離載子分布會呈現非均勻性。入射電磁輻射使矽晶體帶電，導致在位於矽晶體頂部的溝槽底部與晶體底面之間產生較強的電場（即誘發較高的游離載子濃度）。我們模擬了沿矽晶體表面的游離載子濃度再分佈以及該晶體近場區域電場強度。結果顯示，集中於矽晶體溝槽中的高游離載子濃度可促使自發電擊穿，造成電場強度再分佈並沿共振器-轉換器表面產生電流流動[9]。這表示，為了最有效地阻尼特定頻率範圍的電磁波能量，需優化共振器-轉換器中矽晶體的摻雜（即其電導率）。 研究也顯示，谐振器-转换器對電磁輻射（EMR）阻尼的效率，取決於矽晶體與金屬天線的拓撲結構，以及入射電磁輻射的特徵頻率 / 波長。

Due to EMR interaction with both antennas and signals interaction with diffraction grating built on the surface of Si crystal, the signal is back scattered in a form of coherent radiation with the maximal amplitude of the electric field located in the centre of the Si crystal (Fig. 5).

由於電磁輻射與兩個天線的交互作用，以及訊號與構築於矽晶體表面的繞射光柵的相互作用，訊號以相干輻射的形式被向後散射，電場振幅的最大值位於矽晶體的中心（圖 5）。

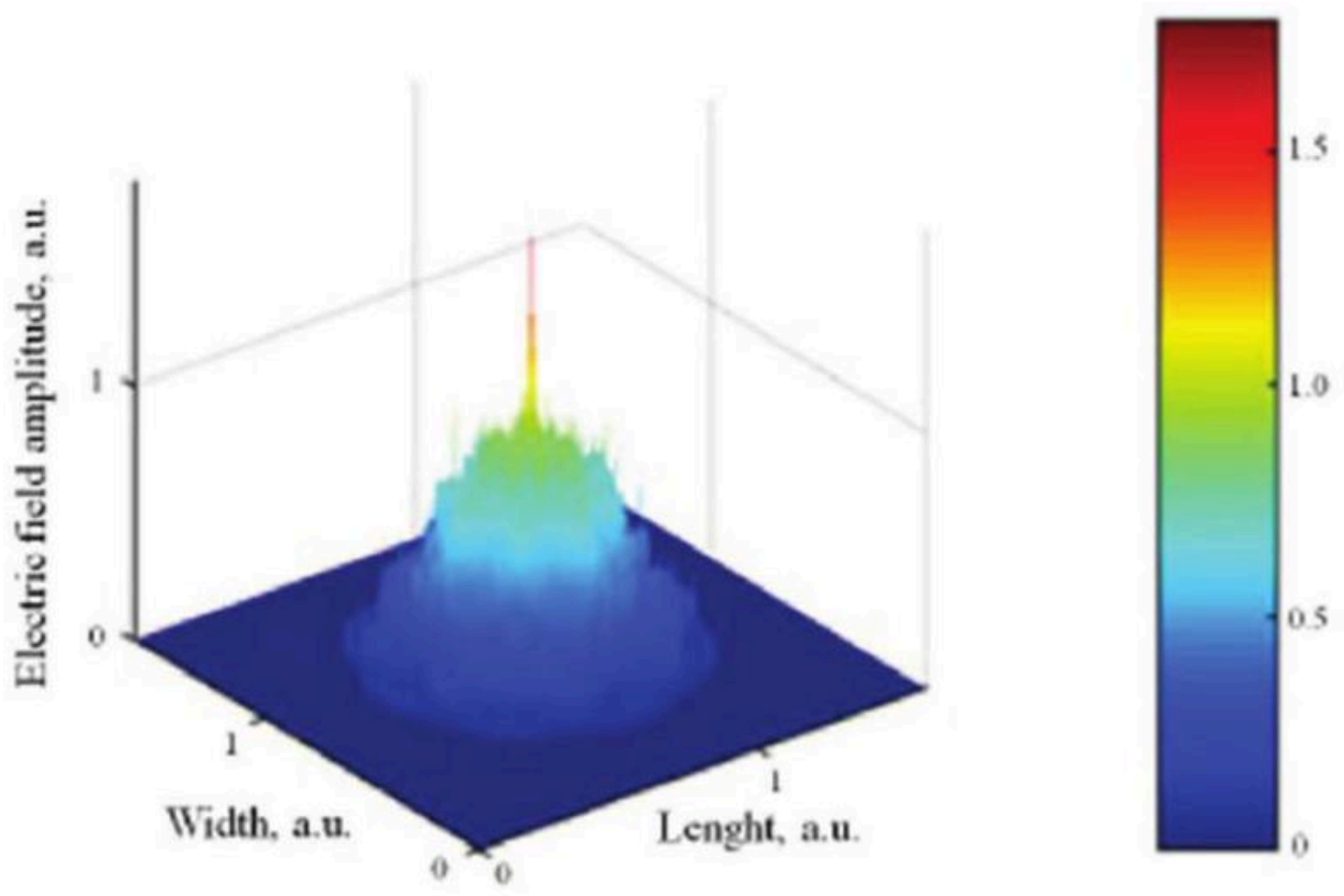

\captionsetup{labelformat=empty}
Figure 5: Fig. 5. The three-dimensional (3D) view of the electric field strength distribution in near-field zone of the 1 mm thick, round (5.75 cm in diameter) shaped Si crystal with plasma-chemically etched $0.5-\mu$m-wide and $0.5-\mu$m-deep grooves of rectangular cross-section on its surface

Figure 5: Fig. 5. 三維視圖（3D）顯示在近場區域內電場強度分布，對象為厚 1 mm、圓形（直徑 5.75 cm）的矽晶體，其表面經等離子化學蝕刻形成寬度為 $0.5-\mu\mathrm{m}$ 且深度為 $0.5-\mu\mathrm{m}$ 的矩形橫截面槽溝。

Increasing power of an incident EMR, a noticeable field amplitude appears also at the crystal edges in such a way producing a bell-like shape of field distribution in the near-field zone of the resonator-converter. The backscattered EMR interfere with incident EMR and the electric field distribution around the resonator-converter surface turns into an intricate three-dimensional (3D) structure [9]. A backscattered signal affects redistribution of electric field amplitude recorded by the signals detected, exhibiting sharp non-linear growth of electric field amplitude starting with the device's antenna edges and spreading towards its center as well as towards the centre of the Si crystal. Our results of numeric simulation show that due

to backscattered wave interference with incident EMR, the frequency of resulting wave could increase for several times and for our tested geometry of Si crystal it increases by 3.2 times [9] in respect to 550 THz frequency of monochromatic EMR from the radiation source.

隨著入射電磁輻射功率增加，在晶體邊緣亦出現明顯的場振幅，從而在諧振器-轉換器的近場區域產生鐘形的場分佈。向後散射的電磁輻射與入射電磁輻射互相干涉，圍繞諧振器-轉換器表面的電場分佈轉變為複雜的三維結構 [9]。向後散射的訊號會影響由探測到的訊號所記錄的電場振幅重新分佈，表現出從裝置天線邊緣開始並向中心以及矽晶體中心擴展的電場振幅急遽非線性增長。數值模擬結果顯示，由於向後散射波與入射電磁輻射的干涉，結果波的頻率可增加數倍，而對於我們測試的矽晶體幾何形狀，相較於來自輻射源的單色電磁輻射 550 THz 頻率，其增加了 3.2 倍 [9]。

Conclusions 結論

The resonator-converter partly suppresses power of incident on it electromagnetic radiation (EMR). The maximal efficiency of signals suppression can be achieved when the resonator-converter is attached directly on a frame or

共振器-轉換器部分抑制作用於其上的電磁輻射（EMR）功率。當共振器-轉換器直接安裝於框架上或

located in a near-field zone of the radiation source, since in the near-field zone is easier to reach and exceed the threshold power $P_{\min}$ necessary for the device's onset.

位於輻射源的近場區時，可獲得最大訊號抑制效率，因為在近場區較容易達到並超過裝置啟動所需的臨界功率 $P_{\min}$ 。

The minimal power needed for the resonator-converter's excitation is $P_{\min} \geq 2\ \mathrm{W}$ measured for the 2.5 GHz frequency radiation source. Our preliminary results also suggest that $P_{\min}$ is a function of antenna and Si crystal surface topology, doping of the Si crystal, and frequency/wavelength of an incident EMR.

對於 2.5 GHz 頻率的輻射源，測得使共振器-轉換器激發所需的最小功率為 $P_{\min} \geq 2\ \mathrm{W}$ 。我們的初步結果也顯示， $P_{\min}$ 為天線與矽晶體表面形貌、矽晶體摻雜以及入射電磁輻射的頻率/波長的函數。

For the case of damping of electromagnetic pollution (EP) (i.e. far-field zone of a radiation source), the maximal damping of EMR power we achieved when the resonator-converter is directly attached to the frame of the signals detector or located at distance shorter or equal to 2λ away from it. Therefore, as a potential protector against EP, the resonator-converter should be used in the near-field zone of signals detector (i.e. human body, shielding electronic device etc.) and/or radiation source (i.e. source of potential EP).

在電磁汙染（EP，亦即輻射源的遠場區）抑制的情況下，當諧振器-轉換器直接附著於訊號探測器的框架上，或位於與其距離小於或等於 2λ 的位置時，我們實現了對電磁輻射（EMR）功率的最大抑制。因此，作為潛在的電磁汙染防護裝置，諧振器-轉換器應用於訊號探測器（例如人體、需屏蔽的電子設備等）和 / 或輻射源（即潛在電磁汙染來源）的近場區域。

Acknowledgements 致謝

Authors A. J and D. J. acknowledges company "Aireslita" UAB and head of the company Mr. Darius Višinskas for the Aires Defenders provided for our experimental measurements.

作者 A. J 與 D. J. 感謝公司 "Aireslita" UAB 及公司負責人 Darius Višinskas 先生，感謝其提供 Aires Defenders 以供我們進行實驗測量。

References 參考文獻

[1] Nguyen VD., Bouisset P., Kerlau G., Parmentier N., Akatov YA., Archangelsky VV., Smirenniy LN., Siegrist M. A new experimental approach in real time determination of the total quality factor in the stratosphere. Rad. Prot. Dos. 1993, 48(1): 41-46.

[1] Nguyen VD., Bouisset P., Kerlau G., Parmentier N., Akatov YA., Archangelsky VV., Smirenniy LN., Siegrist M. 一種在平流層即時測定總品質因數的新實驗方法。Rad. Prot. Dos. 1993, 48(1): 41-46.

[2] Johansen Ch. Electromagnetic fields and health effects - epidemiologic studies of cancer, diseases of the central nervous system and arrhythmia-related heart disease. Scand J Work Environ Health 2004, 30 Suppl 1: 1-80.

[2] Johansen Ch. 電磁場與健康影響——癌症、中樞神經系統疾病與心律不整相關心臟病的流行病學研究。Scand J Work Environ Health 2004, 30 Suppl 1: 1-80.

[3] Hardell L., Sage C. Biological effects from electromagnetic field exposure and public exposure standards. Biomedicine & Pharmacotherapy 2008, 62: 104-109.

[3] Hardell L., Sage C. 電磁場曝露的生物學效應與公共曝露標準。Biomedicine & Pharmacotherapy 2008, 62: 104-109.

[4] Terzia M., Ozberka B., Denizb OG., Kaplanb K. The role of electromagnetic fields in neurological disorders. J. Chem. Neuroanatomy. 2016, 75: 77-84.

[4] Terzia M., Ozberka B., Denizb OG., Kaplanb K. 電磁場在神經系統疾病中的角色。J. Chem. Neuroanatomy. 2016, 75: 77-84.

[5] Repacholi MH., Basten A., Gebski V., Noonan D., Finnie J., Harris AW. Lymphomas in E mu-Piml transgenic mice exposed to pulsed 900 MHz electromagnetic fields. Radiation Research.1997, 147(5): 631-640.

[5] Repacholi MH., Basten A., Gebski V., Noonan D., Finnie J., Harris AW. 在暴露於脈衝式 900 MHz 電磁場之 E mu-Pim1 轉殖小鼠中的淋巴瘤。Radiation Research.1997, 147(5): 631-640.

[6] Phillips JL, Singh NP, Lai H. Electromagnetic fields and DNA damage. Pathophysiology 2009, 16(2-3): 79-88.

[6] Phillips JL, Singh NP, Lai H. 電磁場與 DNA 損傷。Pathophysiology 2009, 16(2-3): 79-88.

[7] Marvin AC., Dawson JF., Ward S., Dawson L., Clegg J., Weissenfeld A. A proposed new definition and measurement of the shielding effect of equipment enclosures. IEEE Trans. Electromag. Compat. 2004, 46(3): 459-468.

[7] Marvin AC., Dawson JF., Ward S., Dawson L., Clegg J., Weissenfeld A. 擬議之設備外殼屏蔽效應之新定義與測量。IEEE Trans. Electromag. Compat. 2004, 46(3): 459-468.

[8] Land SO., Tereshchenko O., Ramdani M., Leferink F., Perdriau R. Proceedings of the International Symposium on Electromagnetic Compatibility (EMC'14/Tokyo), 2014: 777-780.

[8] Land SO., Tereshchenko O., Ramdani M., Leferink F., Perdriau R. 國際電磁相容性研討會（EMC'14/東京）論文集，2014: 777-780。

[9] Kopyltsov AV., Korshunov KA., Lukyanov GN., Serov IN. Distributed Calculations of the Interaction of Electromagnetic Radiation with a Structured Surface//Regional Informatics and Information Security. Collected Papers. Saint Petersburg Society of Computer Science, Computer Hardware, and Communication and Control Systems 2016, 2:383-387.

[9] Kopyltsov AV., Korshunov KA., Lukyanov GN., Serov IN. 分散式計算電磁輻射與結構化表面相互作用 // Regional Informatics and Information Security. Collected Papers. Saint Petersburg Society of Computer Science, Computer Hardware, and Communication and Control Systems 2016, 2:383-387.

Corresponding author. Tel.: +370-5-274-4833; fax: +370-5-274-4844

通訊作者。電話：+370-5-274-4833；傳真：+370-5-274-4844

E-mail address: arturas.jukna@vgtu.lt
** Corresponding author. Tel.: +7-921-401-9427; fax: +7-812-233-7720

**** 通訊作者。電話：+7-921-401-9427；傳真：+7-812-233-7720**

E-mail address: kopyl2001@mail.ru

電子郵件地址：kopyl2001@mail.ru